5 Flow over Inclined Flat Plates

In this work, the experimental investigation of free convection boundary layer over an inclined plate whose inclination varies from 30° to 60° has been carried out. Particle image Velocimetry (PIV) technique was used to determine the flow characteristics over the inclined plates. The influence of various values of the inclination angles and heat fluxes on the flow structure has been examined. Two different flow regimes - laminar and transitional formed over the inclined plates and the results related to them have been presented. The various hydrodynamic parameters such as wall shear stress and velocity boundary layer thickness used for defining or identifying the onset of velocity transition has been discussed.

5.1 Experimental Details

5.1.1 Free convection setup

The free convection VBL over an inclined flat plate with physical coordinate system is shown in figure 5.1. In this study, a plate of length L which is inclined at ϕ degree to the horizontal and subjected to a uniform wall heat flux of q_w'' is considered. The origin O is assumed at the leading edge of the plate. The stream wise distance along the plate from the leading edge and normal distance from the plate are taken as x and y respectively. The x' and y' have been considered to be the coordinates in the horizontal and vertical directions from the origin, respectively. Also, the parallel and perpendicular components of velocity are denoted as u and v respectively.

Figure 5.2(a) shows the schematic diagram of the experimental setup. In the present work, the flow structure to be analysed develops adjacent to the heated inclined plate. The inclined plate assembly with the water tank has been designed to provide an unbounded free convection behaviour. In this work, a brass plate of length 150 mm, width 100 mm and

thickness 0.5 mm was used as a heating surface. A silicon rubber heater was used for heating the brass plate. The plate was attached to the heater with pressure sensitive adhesive, leaving no air gap between plate and heater. For reducing surface reflection during the experiments, the front surface of the plate was spray-painted with matt black [77,78]. A fence of 200 mm height is attached to either side of the plate assembly as can be seen in figure 5.2(a). This has been done to restrict the flow in span wise direction. The plate assembly was kept in a glass tank of dimensions of 600 (x) × 600 (y) × 500 (z) mm with the trailing edge of the plate 280 mm below the free surface of the water and the leading edge 160 mm above the tank bottom wall.

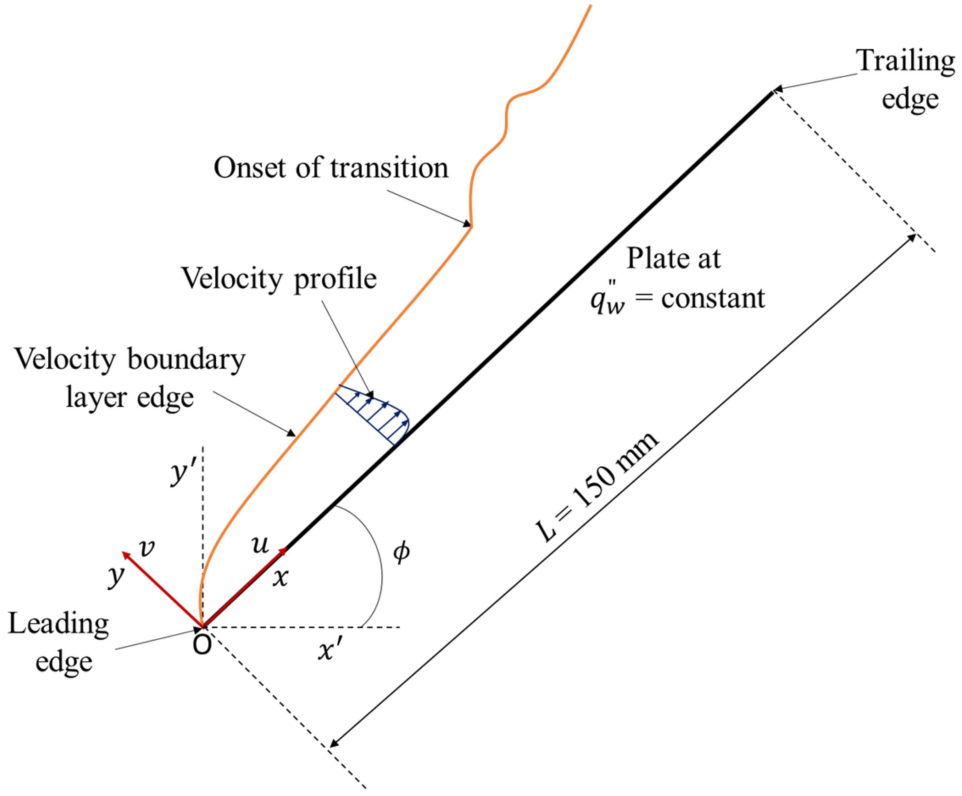

Figure 5.1: Velocity boundary layer over an inclined plate with physical coordinates

Figure 5.2(b) depicts a side view of the inclined plate assembly together with the position of the thermocouples. The temperature of the plate surface and the bulk fluid were

measured using k-type thermocouples of 0.5 mm diameter. All the thermocouples were calibrated using a thermostatic bath and a four wire master RTD having an accuracy of 1/10 DIN. The thermocouples were embedded through the back side of the plate heater assembly and tip of the thermocouples coincides with the front heated surface of the plate. This arrangement ensures that the thermocouples measure the surface temperature accurately and do not disturb the flow over the wall. The thermocouples are located in the middle of the plate and at x = 5 mm, 40 mm, 75 mm, 110 mm and 145 mm as shown in figure 5.2(b). The bulk temperature of water was calculated using the mean readings of three thermocouples located at 143 mm below the leading edge, 65 mm above the leading edge and 263 mm above the trailing edge of the plate respectively, as shown in figure 5.2(b) for 60° inclination. These thermocouples were arranged vertically and spaced 30 mm away from the centre of the plate as illustrated in figure 5.2(b). The 25 mm thick thermal insulation is provided on the back side of the heater to reduce the heat loss from the back side of the plate heater assembly.

In the present work, to reduce the effect of stratification, the bulk fluid temperature was maintained at 23 $\pm$ 0.1 °C before the start of the experiment. This was achieved by feeding the water to the tank with the aid of a thermostatic bath, which supplied water at 23 °C. The tank was filled to the necessary height using this constant temperature water and after that the connection to the bath is removed. To ensure that the bulk fluid temperature does not change, the laboratory temperature has also been maintained around 23 °C throughout the experiment. The thermocouples readings were recorded by a data acquisition system. The top surface of the tank is kept covered by a 20 mm thick thermocal insulation to reduce the effect of evaporation and disturbance from the free surface.

(a)

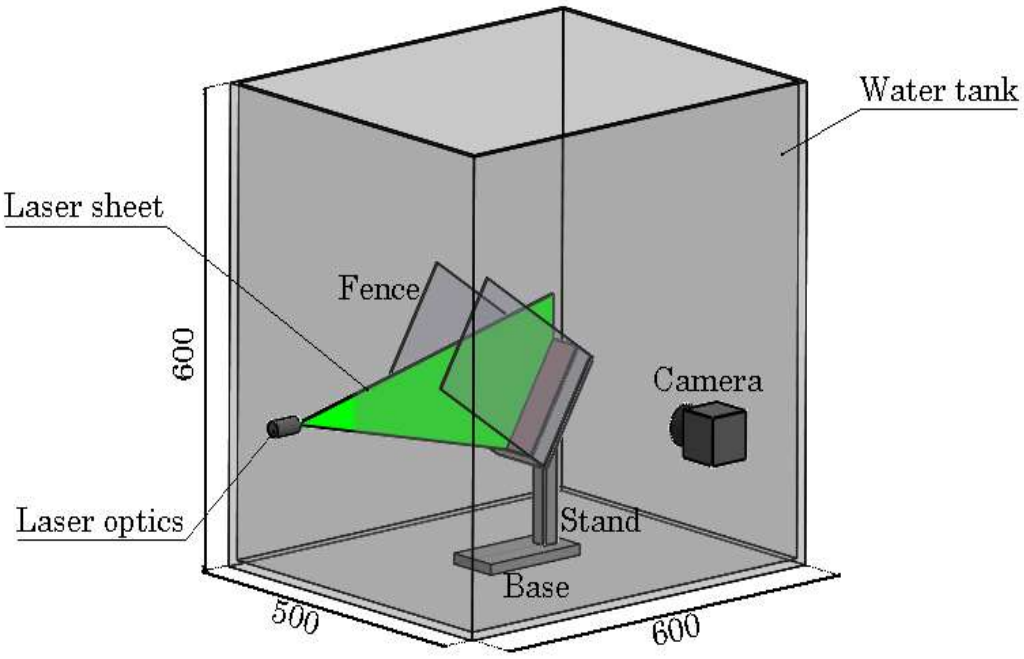
Water tank
Laser sheet
Fence
600
Camera
Laser optics
Stand
Base
500
600

(b)

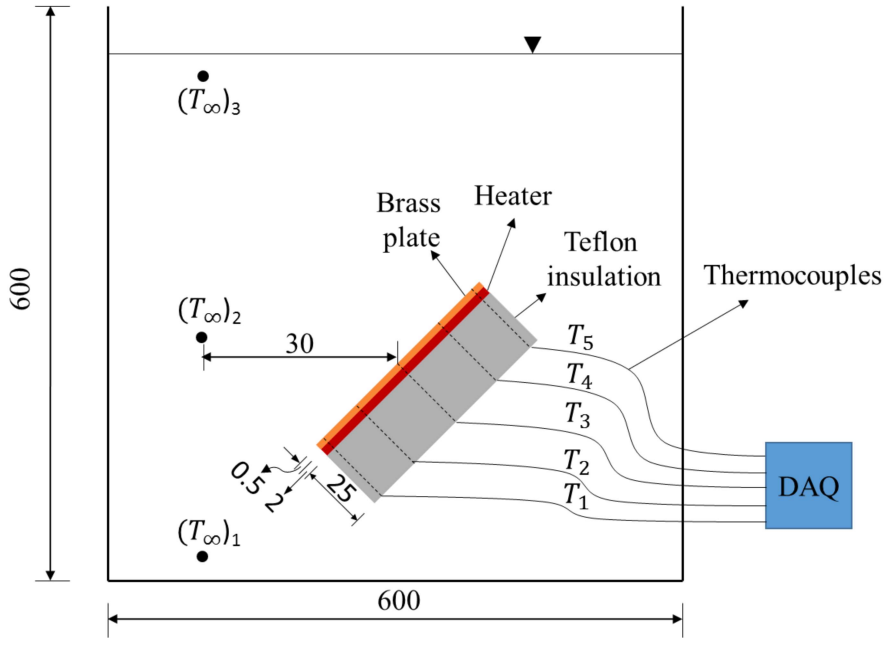
$(T_\infty)_3$
Brass plate
Heater
Teflon insulation
Thermocouples
600
$(T_\infty)_2$
30
T_5
T_4
T_3
T_2
T_1
0.5
2
25
DAQ
$(T_\infty)_1$
600

(c)

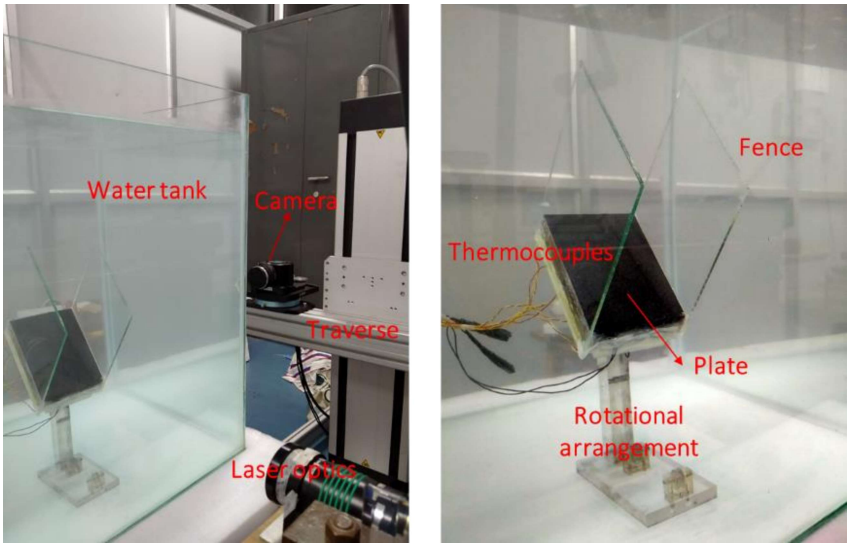

All dimensions are in mm

Figure 5.2:(a) Schematic diagram of the experimental setup and (b) location of the thermocouples relative to the plate for $\theta = 45°$, T_1 to T_5 measure surface temperature and $(T_\infty)_1$ to $(T_\infty)_3$ measure bulk fluid temperature (c) actual experimental set-up

5.1.2 PIV technique for velocity measurement

The position of the camera and laser sheet relative to inclined plate assembly is shown in figure 5.2(a). The PIV setup is explained in section 4.2.2 and illustrated in Table 5.1. In this section, the velocity field was derived using an adaptive correlation with minimum and maximum interrogation area sizes of 16 pixels by 16 pixels and 64 pixels by 64 pixels, respectively and with an overlap of 50%.

Table 5.1: PIV recording parameters

Parameters	Specifications
Field of view	159.1 mm by 159.1mm
Magnification factor (M)	0.09524
Pixel size	7.4 µm
Seeding particles	HGS with mean diameter of 10 µm
Settling velocity of seeding particle	6.13 µm/s
f-number of the lens ($f_{\#}$)	16
Wavelength of the laser light (λ)	532 nm
Particle image diameter (d_{image})	3 pixels
Number of images	1000
Correlation	Adaptive correlation
Final interrogation area	16 pixels by 16 pixels with 50% overlap
Recording method	Single frame
Acquisition rate	15 Hz

5.2 Results and discussion

The objective of the present investigation is to study the flow structures over an inclined plate whose inclinations are 30°, 37°, 45°, 53° and 60° from horizontal. Based on the flow structures, the variation in hydrodynamic characteristics in the streamwise direction have been discussed. Constant wall heat fluxes of 100, 500, 1000, 2000, and 5000 W/m^2 were used in the experiment. In the present work, the average modified Rayleigh numbers (Ra_L^*) based on the length of the plate varies from 7.16×10^8 to 7.90×10^{10}. Here, $Ra_L^* = \frac{g sin\emptyset \beta q_w'' L^4}{\alpha \vartheta k}$ with $\emptyset$ being the angle of inclination of the plate from horizontal, g the

gravitational acceleration, L the length of the plate, q_w'' the wall heat flux, β the thermal expansion coefficient, α the thermal diffusivity, ϑ the kinematic viscosity, and k the thermal conductivity. All these thermo-physical properties were evaluated at the mean film temperature and taken from the book by Bergman et al. [17]. The flat plate with an aspect ratio (length/width) of 1.5 was used in the present investigation. All the results are reported for the mid plane of the inclined plate.

5.2.1 Hydrodynamic characteristics

For the evaluation of hydrodynamic characteristics, the flow structure over the inclined plates have been obtained after image processing of acquired images as discussed earlier. Figure 5.3 shows the u-velocity contours for various inclination of the plate at a heat flux of 1000 W/m^2. The formation of VBL over the inclined plate is clearly seen in figure 5.3. The VBL grows in the streamwise direction due to the entrainment of the bulk fluid into the VBL. An abrupt change in the VBL thickness at a particular streamwise position for plate inclinations of 30° and 45° is seen in figures 5.3(a) and 5.3(b) respectively. This location is seen shifted towards trailing edge when inclination angle increases from 30° to 45°. The results for ϕ = 37° are not shown for clarity. Only a laminar regime present for plate inclination of 53° and 60° as shown in figures 5.3(c) and 5.3(d) respectively. This suggests the occurrence of two distinct regimes-laminar and transition when $30° \leq \phi \leq 45°$.

Figure 5.4 shows the u-velocity profiles at different streamwise locations along the plate for $\phi = 45°$ and at the heat fluxes of 1000 W/m^2 and 2000 W/m^2. It is observed from figure 5.4 that the overall VBL consists of two layers: an inner VBL in which u-velocity increases from zero (no-slip condition at the wall) to a maximum value (u_{max}) and an outer VBL in which the u-velocity asymptotically decreases from u_{max} to a very low value. It can been also seen that the thickness of the inner VBL is very large at x = 100 mm

compared to its thickness at x = 20 mm and 50 mm for both the heat fluxes. A similar drastic increase in the total VBL thickness was observed in figure 5.3(b) around this distance. This demonstrates that not only the total VBL thickness but also the inner VBL thickness can be used as an indicator for the identification of different flow regimes. Hence it can be said that the position x = 100 mm is in the transition region, while the laminar region extends from x = 20 mm to x = 50 mm. The location of the onset of transition would be lying between x = 50 to x = 100 mm. As figures 5.3 and 5.4 depict that the flow regime changes from laminar to transition as fluid flows along the plate for plate inclination $\phi \leq 45$, it is crucial to determine the location of the point where the laminar regimes cease and transition begins. Hence, in the next section, different identification methods for the onset of transition have been discussed.

The effect of heat flux on velocity profile at 45° inclined plate is shown in figure 5.4. Now, figure 5.5 shows the u-velocity profile for various inclined plates at a heat flux of 1000 W/m^2 and x = 50 mm. It is observed that the u-velocity increases with increase of inclination angle at a particular value of x and heat flux. The locus of u_{max} shifts towards the left of the curve which indicates that the magnitude of inner VBL thickness decreases with an increase in the inclination angle. From the figure 5.5, it is also seen that the u-velocity decreases asymptotically from its peak value to a finite value (not equal to zero) in the outer VBL. It is because the flow is not approaching perpendicular to the plate. The value of u-velocity at the edge of VBL (u_e) decreases with an increase in the inclination angle. For example: the value of u_e is around 1.4 mm/s and 0.3 mm/s for 30° and 60° inclined plates respectively.

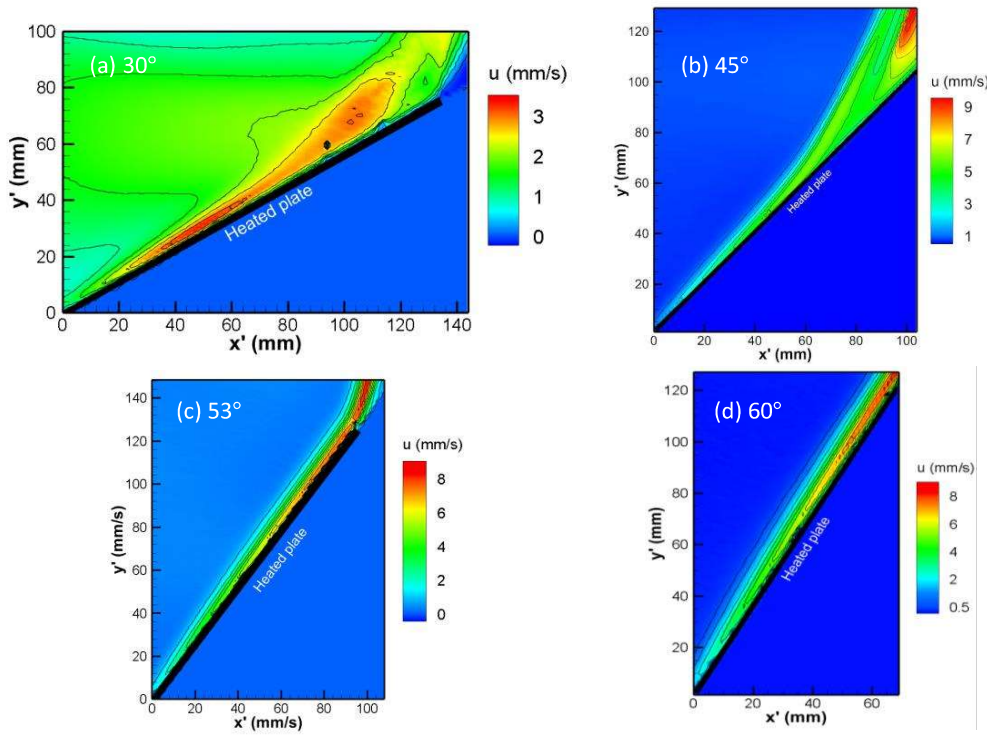

Figure 5.3: *u*-velocity contours at a heat flux of 1000 W/m^2 for plate inclination of (a) 30°, (b) 45°, (c) 53° and (d) 60°

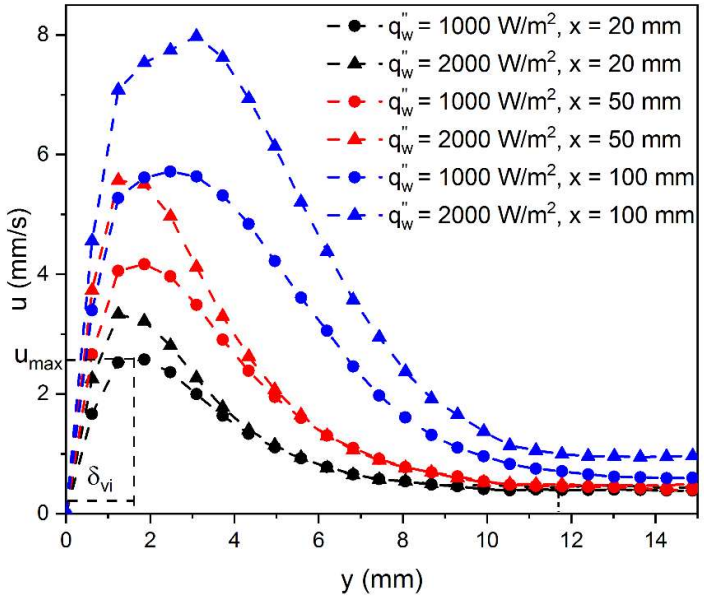

Figure 5.4: u-velocity profile at different streamwise distance along the plate for 45° inclined plate at the heat fluxes of 1000 W/m^2 and 2000 W/m^2

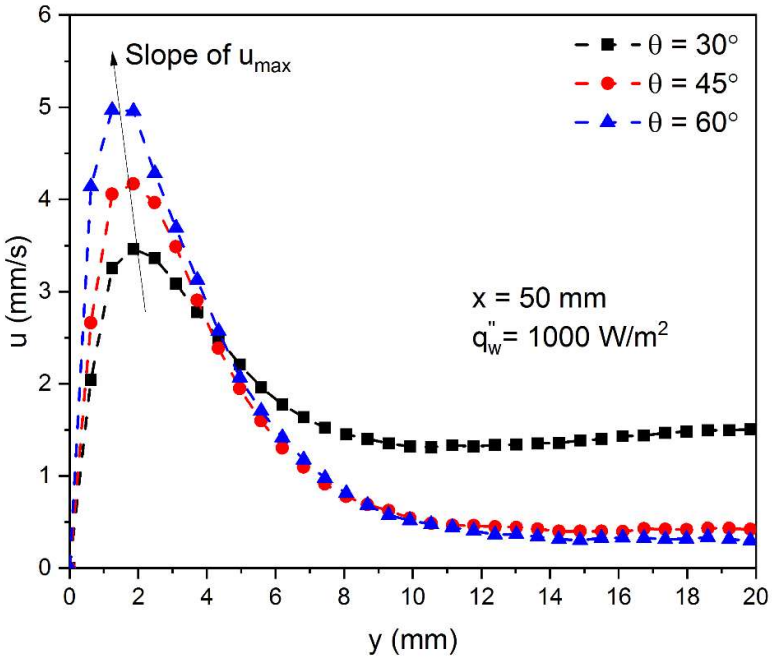

Figure 5.5: u-velocity profile at different streamwise distance along the plate for different inclination of the plate for x = 50 mm and at a heat flux of 1000 W/m^2

5.2.2 Identification of onset of velocity transition

In the previous section, it was found that the two separate regimes (laminar and transition) formed over an inclined plate for inclinations angles less than 45. This section deals with identification of the streamwise location (x_t) where the deviation of the laminar regime occurs. In this section, only the results for the 45° inclined plate are shown for simplicity in presentation. Four indicators have been used to identify the onset of transition point. They are based on the variations of overall VBL thickness (δ_v), inner VBL thickness(δ_{vi}), maximum streamwise velocity (u_{max}) and wall the shear stress(τ_w) with the streamwise distance along the plate. A sharp deviation in these hydrodynamic parameters is considered as an indicator of the onset of transition. Figure 5.6 shows the algorithm for calculating the value of x_t. A code written in MATLAB was used to implement the algorithm. The initial step of the algorithm is to apply a smoothing filter to the experimental data. After that the

range of x between x_{start} to x_{end} was chosen where 'start' and 'end' are the indices of starting and endpoint of streamwise locations. The minimum streamwise distance has been used as the starting point to mitigate the leading edge effect and its value is set as $x_{start} =$ 20 mm in each case. The value of x_{end} was chosen well below the transition regime. A power law fitting of the experimental curve ($E(x)$) from x_{start} to x_{end} has been done and is represented by $y(x)$. The mean absolute deviation (MAD) between fitted $y(x)$ and experimental curve $E(x)$ over the range of x (x_{start} to x_{end}) has been computed as

$$\text{MAD} = \frac{\sum_{i=1}^{i=N} |E(x_i) - y(x_i)|}{N} \tag{5.1}$$

The absolute deviation (AD) is also computed at location x_{end} between $E(x_{end})$ and $y(x_{end})$ as

$$\text{AD} = |E(x_{end}) - y(x_{end})| \tag{5.2}$$

The value of x_{end} has been increased from its previous value until

$$\text{AD} > C \times \text{MAD} \tag{5.3}$$

where C is a constant. Based on the signal to noise ratio of the experimental data, the value of C is set to 5. The position of onset of transition (x_t) is defined as the value of x_{end} when equation 5.3 is satisfied.

a. Based on criterion of overall VBL thickness (criterion (i))

One of the most essential parameters in identifying a transition point in a fluid flow is the thickness of the VBL. When fluid is entrained into the VBL, it grows in the streamwise direction. The transition from laminar to turbulent flow begins when the laminar flow becomes unstable, increasing the disturbances in the boundary layer. It then causes turbulent fluctuations to emerge, which influences the velocity profile and the rate of expansion of the VBL. Also, the concentrated energy in the BL begins to diffuse more rapidly into the bulk fluid, causing a dramatic increase in VBL thickness. The

commencement of the velocity transition can be indicated by a dramatic increase in VBL thickness. Furthermore, the identification of the VBL's edge is essential for the quantitative determination of VBL thickness. In a forced convection scenario, the normal distance from the wall where the streamwise velocity in the direction of flow is 99 percent of free stream velocity is generally designated as the VBL edge. However, because the bulk fluid is stagnant in the case of free convection, the above definition is inadequate for identifying the edge of VBL for a free convection problem. Goodrich et al. [6] have highlighted this research gap and provided a few ways for determining the VBL thickness. They adopted an approach in which the edge of the VBL is considered to be a locus of constant streamwise velocity of 2 mm/sec for all of their experimental conditions. However, when there is a large variation in the heating conditions, as is the case in the present work, this method is not suitable. This is because for small and large values of heat flux, the magnitude of u_c differs significantly. This has been illustrated in figure 5.7 which depicts the u-velocity contour for a 45° inclined plate at lower and higher heat fluxes of 100 W/m^2 and 5000 W/m^2 respectively. In figure 5.7, the coordinate system has been rotated 45° clockwise to make the VBL more visible. It is found from figure 5.7 that the magnitude of u-velocity near the VBL's edge is not of the same order of magnitude for both the heat fluxes. Although the 2 mm/s contour line (as assumed by Goodrich et al. [6]) can be used to represent the VBL's edge for a heat flux of 5000 W/m^2, it cannot be used for a heat flux of 100 W/m^2 where the velocity at the edge is much smaller than 2 mm/s. As a result, in this study, we use a method for the calculation of VBL thickness that takes into account the influence of significant variations in heating conditions. In the present work, the edge of the boundary layer is marked at the location where the streamwise velocity (u_e) is equal to 10% of reference velocity (u_r) i.e.

$$u_e = 0.1u_r \tag{5.4}$$

The reference velocity is computed from scale analysis [4] and is given as

$$u_r = \frac{\alpha}{L}(Ra_L^*)^{2/5} \tag{5.5}$$

where Ra_L^* is the average modified Rayleigh number and α is the thermal diffusivity of fluid.

The values of u_e for heat fluxes of 100 W/m^2 and 5000 W/m^2 are 0.4 mm/s and 2.27 mm/s, respectively, as computed from equations (5.4) and (5.5) and is marked in figure 5.7. Therefore, method of identification of VBL edge is suitable for both higher and lower values of heat fluxes.

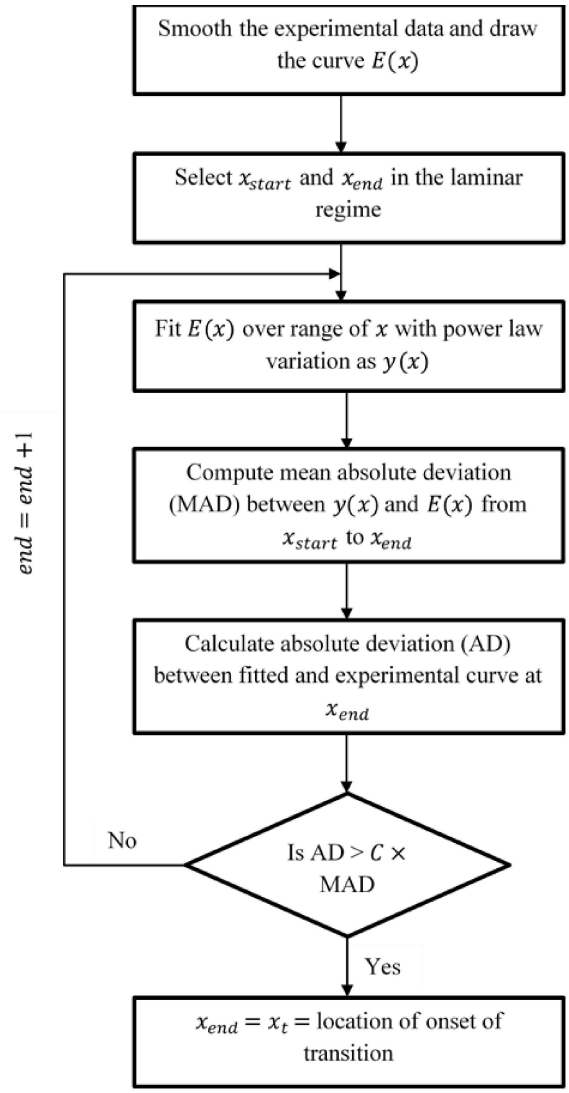

Figure 5.6: Algorithm for identification of onset of transition

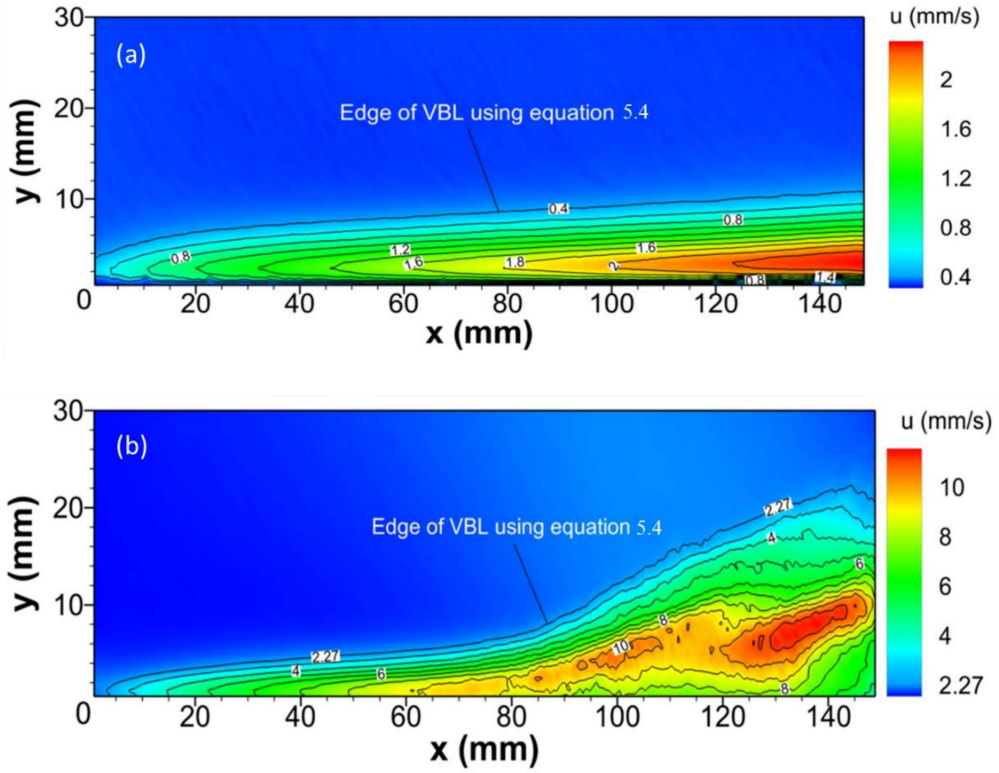

Figure 5.7: u-velocity contour of a 45° inclined plate at the heat fluxes of (a) 100 W/m^2 and (b) 5000 W/m^2 (coordinates system with plate were rotated by 45° clockwise for clear visualisation of VBL)

Figure 5.8 depicts the variation of overall VBL thickness in the streamwise direction for a 45° inclined plate and at heat fluxes of 500 W/m^2 and 5000 W/m^2. It is seen that in the laminar region, the VBL thickness increases at a steady rate in the streamwise direction, but then increases abruptly when the transition from laminar to turbulent begins. The algorithm in figure 5.6 has been used to determine the location at which the thickness of the VBL begins to deviate from the laminar trend in the streamwise direction from the leading edge. Moreover, the commencement of transition is found to be shifted upstream as the heat flux increases. It is because with an increase in heat flux the thermal instability increases. For instance, the estimated distance from the leading edge in the streamwise direction for the onset of transition per unit length of the plate (x_t/L) based on the VBL

thickness criteria for the heat fluxes of 500 W/m^2 and 5000 W/m^2 are 0.65 and 0.43 respectively. It is also found that in the laminar regime, VBL thickness decreases with the increase of heat flux.

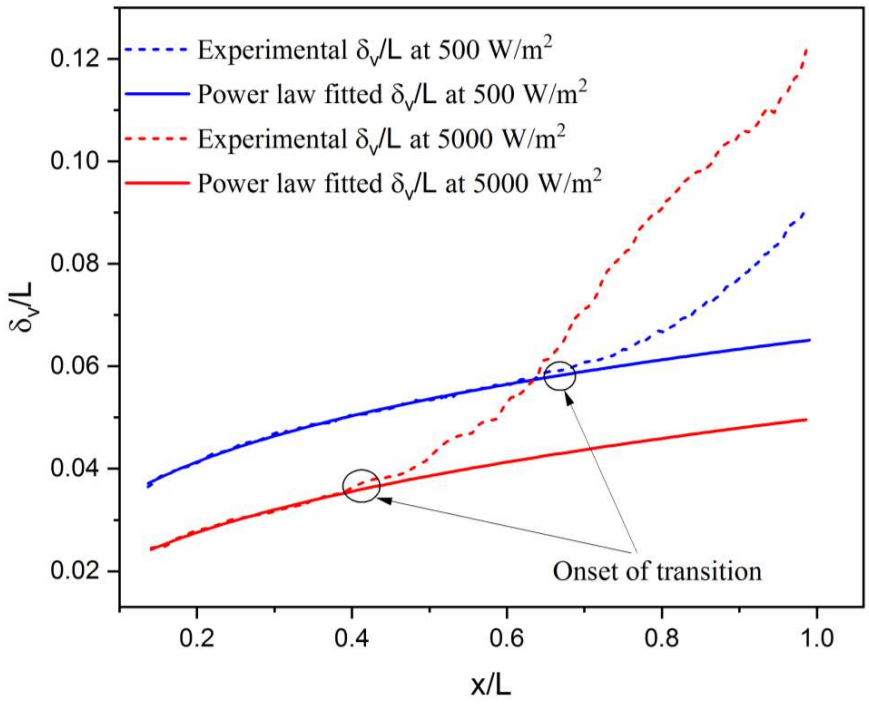

Figure 5.8: Variation of overall VBL thickness in streamwise direction for a 45° inclined plate and at the heat fluxes of 500W/m^2 and 5000 W/m^2

b. Based on criterion of inner VBL thickness (criterion (ii))

The variation of overall VBL thickness was mentioned in the previous section. In this section, the variation of only inner VBL thickness for flow over an inclined plate has been examined. Inner VBL thickness is the normal distance from the wall to the location of u_{max} which is experimentally determined. As a result, unlike the previous method, this method does not require a separate procedure for determining reference velocity. Also, the thickness of the inner VBL is crucial in determining the wall shear stress. Figure 5.9 shows the variation of inner VBL thickness with the streamwise distance along the plate at heat fluxes of 500 W/m^2 and 5000 W/m^2. A slow rise in the inner VBL thickness in the laminar

regime is observed when compared to the overall VBL thickness (Figure 5.8). For example, from $x/L = 0.20$ to 0.33, the increase in inner and overall VBL thickness are 1.90% and 16.95%, respectively for a heat flux of 500 W/m^2. The transition from laminar to turbulent began when the inner VBL thickness increases suddenly, as seen in figure 5.9. The algorithm in figure 5.6 is used to determine the value of x_t. The beginning of transition is found to be shifted upstream as the heat flux increases, similar to case of overall VBL thickness. For example, the value of x_t/L for the heat fluxes of 500 W/m^2 and 5000 W/m^2 are 0.69 and 0.48 respectively. It is also seen that in laminar regime, the inner VBL thickness decreases with the increase of the heat flux similar to VBL thickness.

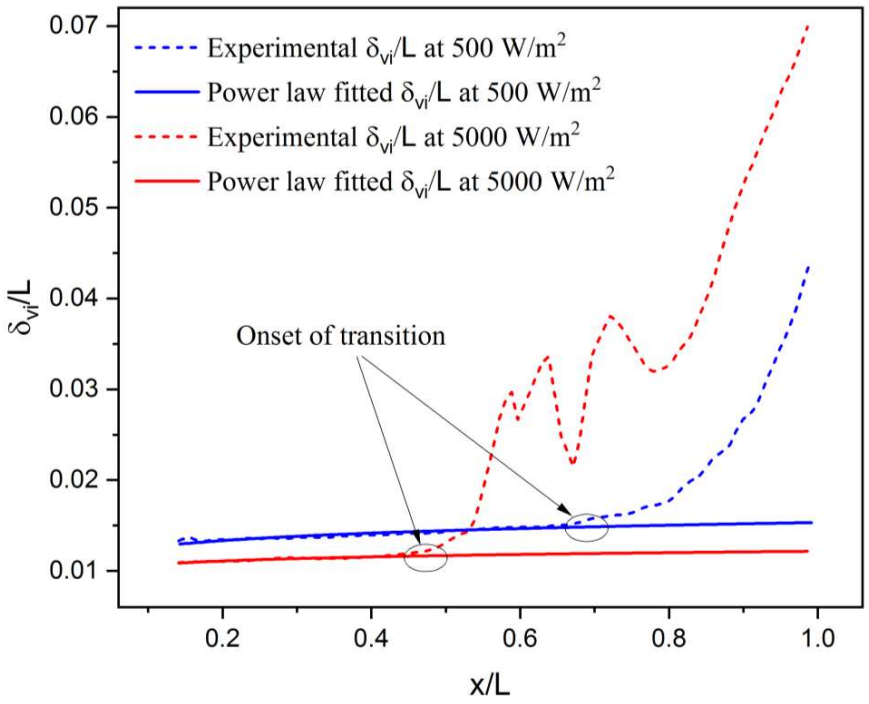

Figure 5.9: Variation of inner VBL thickness along the length of the plate for a 45° inclined plate and at the heat fluxes of 500 W/m^{2}and 5000 W/m^2

c. Based on criterion of maximum u-velocity (criterion (iii))

In this criterion, instead of tracking the location of u_{max}, the variation in u_{max} for flow along the streamwise direction has been evaluated. Figure 5.10 shows the variation of u_{max}

with x for the heat fluxes of 500 W/m^2 and 5000 W/m^2. From figure 5.10, it is observed that the u_{max} increases with x in the laminar region with power law variation, but it starts to deviate from this trend after a specific location in the flow direction. The commencement of the transition is again indicated by algorithm mentioned in figure 5.6. The beginning of transition is found to be shifted upstream as the heat flux increases, similar to previous criteria. For example, the values of x_t/L for the heat fluxes of 500 W/m^2 and 5000 W/m^2 are 0.71 and 0.49 respectively. It is also observed that in laminar regime, the u_{max} increases with the increase of the heat flux.

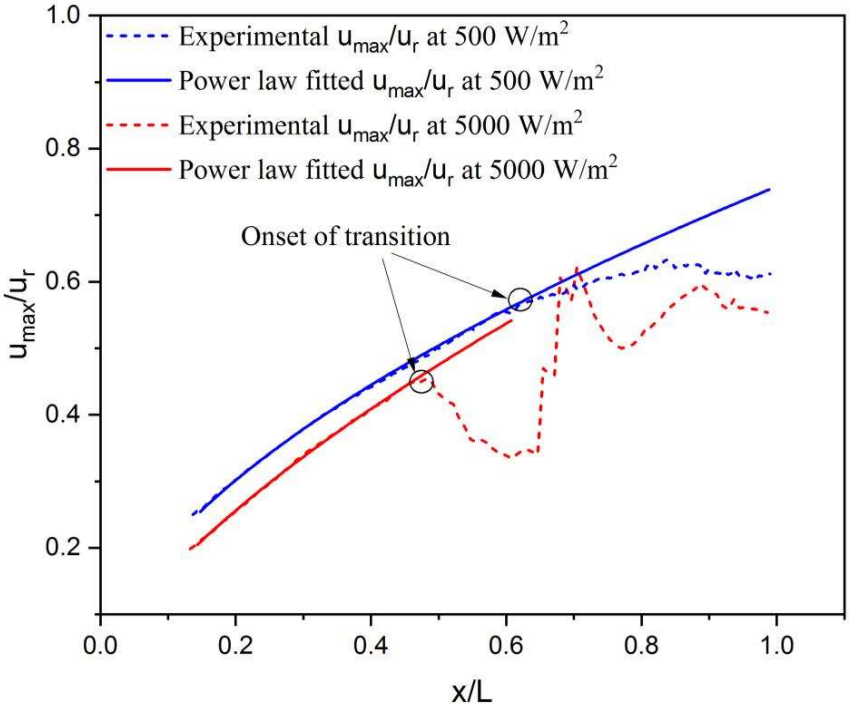

Figure 5.10: Variation of maximum u-velocity in the VBL along the length of the plate for a 45° inclined plate and at the heat fluxes of 500 W/m^2 and 5000 W/m^2

d. Based on criterion of wall shear stress (criterion (iv))

The formation of the VBL causes a velocity gradient at the wall which generates a wall shear stress. The wall shear stress is calculated as

$$\tau_w = \mu \left(\frac{\partial u}{\partial y}\right)_{y=0} \tag{5.6}$$

where $\left(\frac{\partial u}{\partial y}\right)_{y=0}$ is the velocity gradient at the wall and is evaluated by curve fitting the inner layer data of velocity profile shown in figures 5.4 and 5.5. Figure 5.12 shows the variation of skin friction coefficient ($c_{fx} = \frac{\tau_w}{1/2\rho(u_r)^2}$) with the streamwise distance along the plate. It can be observed from figure 5.11 that the skin friction coefficient increases in the flow direction in the laminar region. It is because in the laminar regime, the increase in u_{max} is more as compared to inner VBL thickness in the streamwise direction (figures 5.9 and 5.10). At the inception of transition, due to an abrupt increase in inner VBL thickness, skin friction coefficient decreases as shown in figure 5.11. The drop in wall shear stress at the beginning of transition for vertical plate is also reported in other studies [35,88]. The streamwise location of onset of transition is calculated using the algorithm depicted in figure 5.6. The value of x_t/L for the heat fluxes of 500 W/m^2 and 5000 W/m^2 are 0.69 and 0.47 respectively.

5.2.3 Comparison of different criteria

Figure 5.12 shows how the streamwise location of onset of transition varies with different heat fluxes for all of the previously stated criteria of identification of point of transition. The transition begins early in the streamwise direction as the heat flux increases. This is due to the fact that the instability rises as the heat flux increases. Also, the early commencement of transition is seen when it is estimated based on the variation of VBL thickness (criterion (i)) for all values of heat fluxes as shown in figure 5.12. This means that the initiation of transition is first felt in the outer VBL and then moves to the inner VBL. This is analogous to the vertical plate situation, where disturbance originates in the bulk fluid and then propagates from the outer to the inner VBL [39]. It is also observed

from figure 5.12 that the transition in inner VBL thickness, wall shear stress and maximum streamwise velocity occurs at a higher value of x_t. Because all of these methods are primarily influenced by the inner velocity profiles. As an early transition is detected using the VBL thickness criterion, it is appropriate to employ this criterion to identify the onset of transition. However, the magnitude of VBL thickness depends on the criterion chosen for identification of VBL edge. For example, if $u_e = 0.2u_r$ is taken as the criterion instead of $u_e = 0.1u_r$ (used in the present work), the values of VBL thickness are different. Therefore, in the present work, the onset of transition is identified and evaluated based on the variation of u_{max} (criterion (iii)).

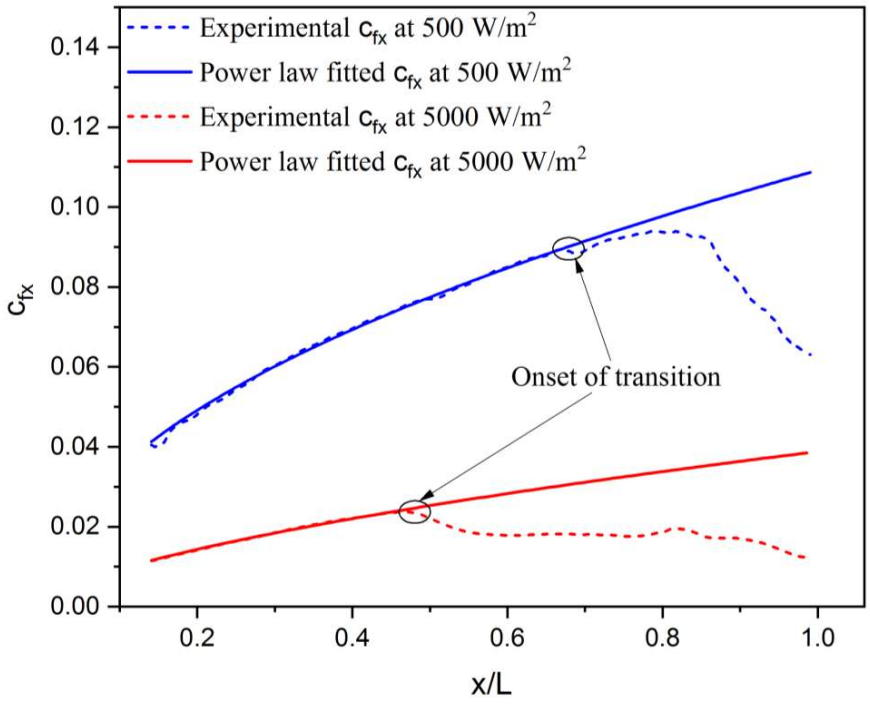

Figure 5.11: Variation of skin friction co-efficient (c_{fx}) with the streamwise distance along the length of the plate for a 45° inclined plate and at the heat fluxes of 500 W/m^2 and 5000 W/m^2

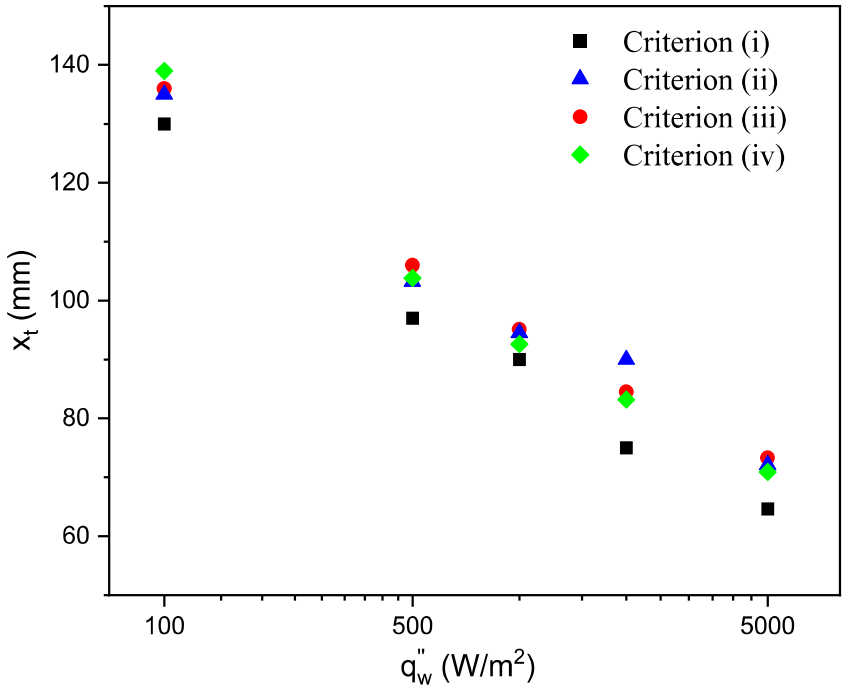

Figure 5.12: Variation of onset of transition (x_t) for a 45° inclined plate evaluated based on the criteria (i) to (iv) with various values of heat fluxes

Figure 5.13 depicts the magnitude of the transition point determined using criterion (iii) mentioned above for different plate inclinations and heat fluxes. The value of x_t increases with ϕ and decreases with q''_w, as seen in figure 5.13. This indicates that as heat flux increases, the transition occurs earlier in the streamwise direction. It is because the thermal instability increases with the increases of heat flux. Also, onset of transition is delayed with the increase in angle of inclination from the horizontal. It is because the buoyancy component along the *plate* increases as the inclination increases. The highest value of $x_t = 136$ mm, is found at $\phi = 45°$ and $q''_w = 100$ W/m^2 and the corresponding Ra^*_x is 7.27×10^8. The smallest value of x_t obtained for $\phi = 30°$ and $q''_w = 5000$ W/m^2 is 41 mm which corresponds to Ra^*_x of 3.09×10^8.

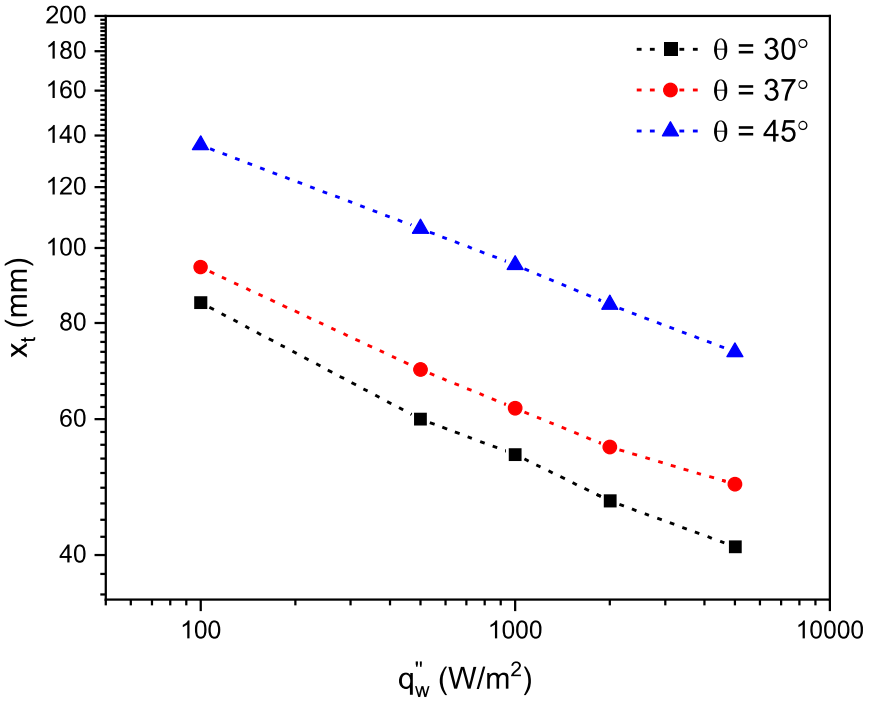

Figure 5.13: Variation of location of onset of transition (x_t) with q''_w for different inclination of the flat plate

5.2.4 Wall shear stress

The variation of τ_w with streamwise direction for a heat flux of 1000 W/m^2 at various inclination angles of plate is shown in figure 5.14. It is clear from the figure that the wall shear stress rises when the inclination of the flat plate from horizontal increases. Additionally, when the inclination angle is increased, the peak of the τ_w moves to the right of the curve. It shows that the inclination angle causes the transition point to move downstream. For 60° inclined plate, the wall shear stress increases continuously in the streamwise direction as shown in figure 5.14. It is because only laminar flow presents for plate inclination of 60°.

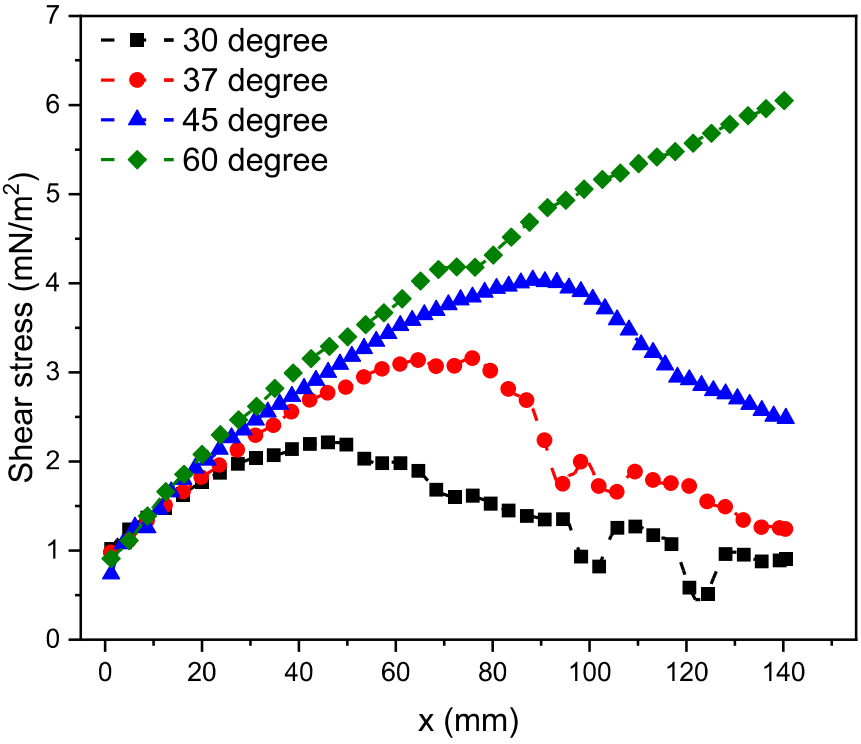

Figure 5.14: Variation of shear stress for different inclination of the flat plate at a heat flux of 1000 W/m^2

5.2.5 Thermal characteristics

The velocity and temperature fields are interdependent in free convection, making it a coupled phenomenon. So, the hydrodynamic characteristics are influenced by the temperature of the plate. The surface temperature measurements taken at various points along the plate at different heat fluxes is used to calculate the local Nusselt number as

$$Nu_x = \frac{h_x x}{k} = \frac{q''_w x}{k(T_w - T_\infty)} \tag{5.7}$$

The Nusselt number is the most commonly used metric for assessing thermal performance. Figure 5.15 shows the variation of local Nusselt number (Nu_x) with local modified Rayleigh number (Ra_x^*) for the 45° inclined plate. Similar to Reynolds number in forced convection, Rayleigh number is a crucial parameter in free convection. Here, $Ra_x^* =$

$\frac{gsin\theta\beta q''_w x^4}{\alpha\vartheta k}$, the gravity component is taken resolved parallel to the plate. Figure 5.15 shows that the Nu_x increases as the Ra_x^* increases, indicating that heat transfer from the plate to the bulk fluid increases. The experimental value of Nu_x closely reflects the correlation proposed by Vliet et al. [42] in the laminar regime as shown in figure 5.15. The commencement of the thermal transition in their work occurs at about $Ra_{cr}^* \sim 10^9$ which they indicated by a departure in Nu_x values from the corresponding values in laminar region. However, the exact position where the thermal transition begins is difficult to identify because this method of determining Ra_{cr}^* corresponding to the onset of transition relied on visual examination of data on a plot of Nu versus Ra_L^* [6]. It is also important to note that the onset of transition is indeed very sensitive to external perturbations. As stated by previous researchers, fluid stratification is the primary reason for inconsistencies in the experimental data [88,89]. For example, in the experiment of Tsuji et al. [88], the temperature gradient in the bulk fluid was about 0.50 to 0.70 °C/m, whereas it was approximately 1.8 °C/m in the experiment of R. Cheesewright [35]. Therefore, the current experiment was performed in such a way that the change in bulk fluid temperature in the vertical direction is kept as small as possible. For instance, before carrying out the experiment, the laboratory and bulk fluid temperatures are held constant at 23 °C for a very long time. The surface and bulk fluid temperatures were monitored during that period, and the experiment was started once it was confirmed that there was minimal variance in all of these thermocouple readings. The maximum increase in bulk fluid temperature in the vertical direction in this work was measured at about 0.56 °C/m. The range of Ra_{cr}^* values corresponding to the commencement of velocity transition estimated from criterion (iii) is also shown in figure 5.15. The minimum and maximum values of Ra_{cr}^* are for 45° inclined plate obtained at 100 W/m^2 and 5000 W/m^2 and its corresponding values are 7.27×10^8

and 4.51×10^9 respectively. Most heat transfer textbooks, on the other hand, assume the transition to begin at a specific value of Ra^*_{cr} [17,20].

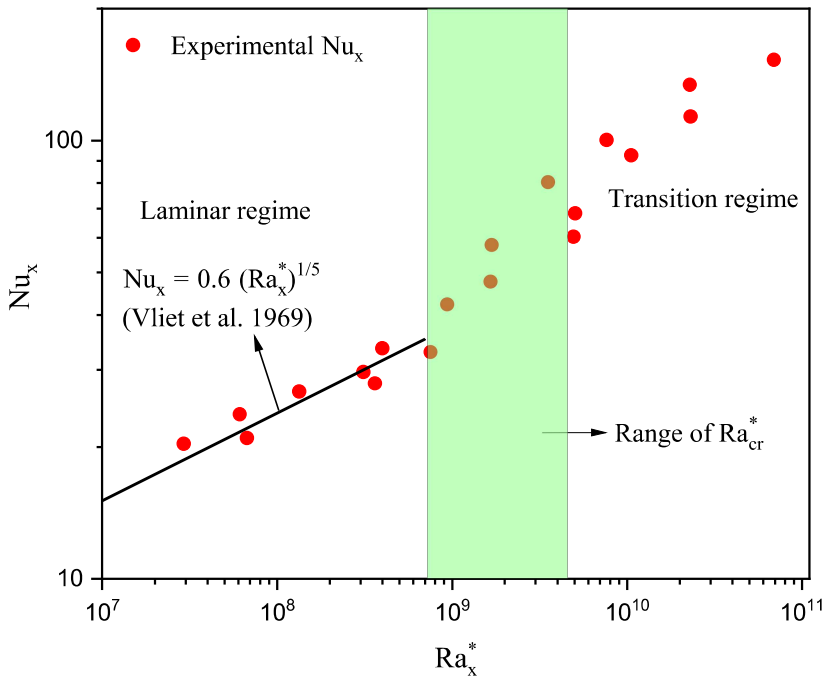

Figure 5.15: Variation of local Nusselt number with modified local Rayleigh number for 45° inclined plate (rectangle shows the range of Ra^*_{cr} obtained from onset of transition identified based on u_{max})

From the present work, it is evident that the transition point for flow along the inclined plate varies with heat flux. Similar type of observation was made in the studies of free convection over a vertical flat plate [36,39,40]. Sevillano et al. [90] experimentally studied the onset of turbulence on inclined plates in free convection. They also found that onset of turbulence depends not only on the Grashof number.

5.3 Conclusion

In the present work, the onset of velocity transition in free convection over an inclined plate whose inclination varies from 30° to 60° has been investigated experimentally. Experiments were performed on a 150 mm long brass plate and subjected to a uniform heat

fluxes in the range of 100 W/m^2 to 5000 W/m^2. It is found that the transition occurs when the inclination of the plate $\theta \leq 45°$. The region where the velocity transition occurs is identified based on the flow structure obtained by PIV technique. Four criteria for the identification of onset of transition - (i) variation of the overall VBL thickness, (ii) inner VBL thickness, (iii) maximum streamwise velocity in the VBL and (iv) wall shear stress have been discussed. The deviation of these parameters from the laminar regime is the indication of onset of velocity transition. It is observed that the initiation of transition is first seen in the overall VBL thickness. However, variation in u_{max} is the most appropriate method for the identification of onset of transition. It was found that the streamwise distance of the onset of velocity transition from the leading edge decreases with the increase of heat flux and increases with the inclination angle. The critical Rayleigh numbers for the onset of transition under various heating conditions have been reported.The highest value of $x_t = 136$ mm, is found at $\theta = 45°$ and $q''_w = 100$ W/m^2 and the corresponding Ra_x^* is 7.27×10^8. The smallest value of x_t obtained for $\theta = 30°$ and $q''_w = 5000$ W/m^2 is 41 mm which corresponds to Ra_x^* of 3.09×10^8. The wall shear stress increases and inner VBL thickness decreases with the increases in inclination angle respectively.